

## Research Article

# Role of Glass Composition on Mechanical Properties of Shape Memory Alloy-Metallic Glass Composites

**Supat Chupradit** <sup>1</sup>, **Indah Raya**,<sup>2</sup> **Dinh Tran Ngoc Huy**,<sup>3,4</sup> **Dmitry Bokov** <sup>5</sup>,  
**Pham Van Tuan**,<sup>6</sup> **Aravindhan Surendar** <sup>7</sup>, **Doaa Alaa Lafta**,<sup>8,9</sup> **Mustafa M. Kadhim**,<sup>10,11</sup>  
**Olga Kravchenko**,<sup>12</sup> **Yasser Fakri Mustafa** <sup>13</sup>, **Zaid Hameed Mahmood**,<sup>14</sup>  
and **Sami Sajjadifar** <sup>15</sup>

<sup>1</sup>Department of Occupational Therapy, Faculty of Associated Medical Sciences, Chiang Mai University, Chiang Mai 50200, Thailand

<sup>2</sup>Department of Chemistry, Faculty of Mathematics and Natural Science, Hasanuddin University, Makassar, South Sulawesi 90245, Indonesia

<sup>3</sup>Banking University HCMC, Ho Chi Minh City, Vietnam

<sup>4</sup>International University of Japan, Niigata, Japan

<sup>5</sup>Institute of Pharmacy, Sechenov First Moscow State Medical University, Moscow 119991, Russia

<sup>6</sup>National Economics University (NEU), Hanoi, Vietnam

<sup>7</sup>Department of Pharmacology, Saveetha Dental College and Hospital, Saveetha Institute of Medical and Technical Sciences, Chennai, India

<sup>8</sup>College of Petroleum Engineering, AL-Ayen University, Thi-Qar, Iraq

<sup>9</sup>Department of Dentistry, Kut University College, Kut, Wasit 52001, Iraq

<sup>10</sup>College of Technical Engineering, The Islamic University, Najaf, Iraq

<sup>11</sup>Department of Pharmacy, Osol Aldeen University College, Baghdad, Iraq

<sup>12</sup>Department of Legal and Social Sciences, Kazan Federal University, Kazan, Russia

<sup>13</sup>Department of Pharmaceutical Chemistry, College of Pharmacy, University of Mosul, Mosul, Iraq

<sup>14</sup>Chemistry Department, College of Science, Diyala University, Baqubah, Iraq

<sup>15</sup>Department of Chemistry, Payame Noor University, PO BOX 19395-4697, Tehran, Iran

Correspondence should be addressed to Sami Sajjadifar; [ss\\_sajjadifar@yahoo.com](mailto:ss_sajjadifar@yahoo.com)

Received 1 November 2021; Revised 8 December 2021; Accepted 15 December 2021; Published 26 December 2021

Academic Editor: Hongchao Kou

Copyright © 2021 Supat Chupradit et al. This is an open access article distributed under the Creative Commons Attribution License, which permits unrestricted use, distribution, and reproduction in any medium, provided the original work is properly cited.

In this work, the molecular dynamics (MD) simulation was applied to design a laminated composite structure comprised of the shape memory alloy (SMA) and Cu-Zr metallic glasses (MGs). A wide range of MG compositions was considered to tune the mechanical features and improve the homogenous plastic deformation during the tension loading. The results indicated that the martensitic transformation in the SMA inhibited the sudden shear band propagation in the composite for all the samples. Moreover, it was revealed that the mechanism of plasticity was significantly affected by the change of MG composition. In the Cu-rich MGs, the formation and propagation of thick shear bands occurred at the end of the tension loading; however, the increase in Zr content induced the interaction of multiple shear bands with finer configurations in the system. Nevertheless, the excessive Zr addition in the MG composition facilitated the aggregation of nanopores at the interface of SMA and MGs, which may be due to the softening effect in the Zr-rich MGs. Finally, it is concluded that an optimized MG composition is required for the trade-off between the plasticity and the strength in the SMA-MG composites.

## 1. Introduction

The design and fabrication of modern engineering materials are resulted from the optimization of various mechanical features such as elasticity, ductility, and strength [1–3]. In the case of metallic glasses (MGs), the superior strength comes at the expense of homogenous plasticity, especially at the tensile mode [4–6]. Hence, it is crucial to strike a balance between the strength and plasticity in the MGs. In general, the localized nanoscale deformation of MGs induces narrow shear bands in the microstructure, leading to a poor homogenous plasticity with a potential catastrophic failure [7]. Thanks to several methods such as microalloying process and rejuvenation [8–12], introduction of the second metallic phase/particle into the glassy matrix has been one of the efficient techniques for hindering the brittle failure. In the metallic glass composites (MGCs), the embedded crystalline phase intensifies the structural heterogeneity in the glassy matrix and improves the plastic deformation through the increase of amorphous/crystalline interfaces [13, 14].

There are several works studying on the mechanism of plastic deformation and strengthening behavior in the MGCs [15–18]. To provide some examples, Zhang et al. [19] indicated that the stress-induced transformation of the crystalline phase in a Ti-based MG improved the strain hardening capability and the resistance to the main shear band propagation. Cheng et al. [20] proposed a novel core-shell structure-reinforced Zr-based MGC with the good tensile ductility and high strength. They found that the simultaneous formation of  $\alpha$ -Zr core and  $\beta$ -Zr shell in the glassy structure was the main reason for improving the mechanical properties. Lyu et al. [21] reported that the precipitation of the crystalline  $\omega$ -Ti phase from the metastable  $\beta$ -type phase under the heating process led to the anomalous increase of storage modulus in  $\text{Ti}_{45.7}\text{Zr}_{33}\text{Cu}_{5.8}\text{Co}_3\text{Be}_{12.5}$  amorphous alloy. In another work, it was revealed that the type of shear bands was not related to the volume fraction of the crystalline phase [22]. Moreover, the propagation of shear bands was mainly controlled by the stress affected zones at crystal/glass interface. Using the selective laser melting process, the ZrCu MGCs reinforced with B2 austenite phase was fabricated, and it was found that the martensitic transformation from the B2 to B19 phase significantly enhances the ductility in the material [23].

Recently, some works have been also carried out to provide a new perspective for the performance of shape memory alloys (SMAs) as the embedded constitute in the glassy matrix [24–27]. In general, the stress-induced martensitic transformation in the SMAs increases the superplasticity and improves the ductility in the SMA-MGCs [25, 28]. To describe with some examples, it was found that the porous NiTi SMA in the Mg-based MG matrix inhibited the rapid propagation of shear bands and improved the plastic strain and fracture strength [29]. In another study, it was suggested that the synergistic influence of elastic excitation in transformed martensite of SMA particles induced the work hardening in the uniaxial response of SMA-MG composites [30]. Using molecular dynamics (MD) simulation, Sopyu et al. [31] unveiled that the deformation

mechanism in the SMA-MG laminated composites included a martensitic transformation, which altered the morphology and propagation of shear bands and stabilized the plastic flow in the body of material. They also showed that the nanowire SMAs could improve the mechanical properties of MGs through the elastic energy release of martensitic transformation [32]. Yuan et al. [33] demonstrated that the brick and mortar designs of SMA-MG composites led to the significant enhancement of tensile ductility.

As depicted, the recent studies have tried to elaborate the mechanism of deformation and mechanical response of SMA-MG composites; however, there is still a long way to identify the detailed features of plasticity in these types of composites. One of the ignored issues is to tune the composition of MGs for obtaining the optimized plasticity-strength in the composite. Hence, in this work, we used the MD simulation to show how the chemical composition of MG affects the mechanism of plasticity in the SMA-MG system. The outcome of this study may provide some guidance for the fabrication of novel composite with optimized plasticity-strength state.

## 2. Computational Method

In the MD simulation, a laminated SMA-MG composite was designed to characterize the plasticity and mechanical properties under the change of MG composition. Here, the crystalline B2-CuZr was considered as the SMA and  $\text{Cu}_{50}\text{Zr}_{50}$ ,  $\text{Cu}_{54}\text{Zr}_{46}$ ,  $\text{Cu}_{60}\text{Zr}_{40}$ , and  $\text{Cu}_{64}\text{Zr}_{36}$  compositions were the glassy alloys. As illustrated in Figure 1, the SMA-MG composite with the amorphous-crystalline interface perpendicular to the tensile direction is designed for the plasticity and mechanical evaluation. In this case, the MG alloy in the form of a cube with 8120 atoms is firstly relaxed at 2200 K for 0.3 ns under the 3D periodic boundary conditions. Afterwards, a quench treatment with the cooling rate of  $10^{11}$  K/s and zero external pressure was performed to make a glassy state in the atomic configuration. Moreover, the sample was kept at 50 K to reach a stable state. The size of cube sample was  $4.1 \text{ nm} \times 8 \text{ nm} \times 3.2 \text{ nm}$ ; however, the replication process was carried out to enlarge the final size of glassy alloy. To avoid any possible void or induced stress in the glassy system, a heating process to 700 K and an aging treatment for 0.3 ns along with a subsequent quench treatment ( $10^{11}$  k/s) were also conducted. Thereafter, the SMA was implemented under the orientations of X-[100], Y-[010], and Z-[001] and merged into the glassy system. In the MD simulation, the MG and SMA systems were combined together, where the interface was built at the (1 0 0) plane of crystalline alloy. Moreover, the SMA-MG system was heated to 700 K with the heating rate of  $10^{11}$  K/s, stabilized for 0.3 ns, and then annealed at 350 K to eliminate any structural defects and interface misalignments. It should be noted that the volume fractions of SMA and MG phases were the same in our alloying system. The detailed size of laminated composite is also given in Figure 1. In this work, the Mendelev embedded atomic potential was used for implementing the MD model through the description of interatomic interactions in the Zr-Cu system [34]. The Mendelev

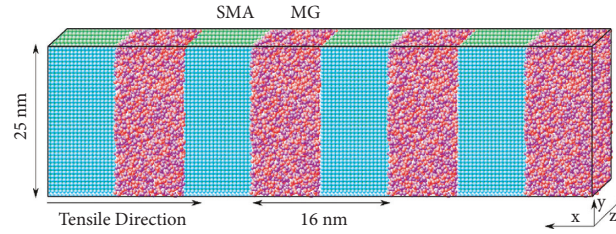


FIGURE 1: The schematic of laminated composite composed of MG and SMA parts.

atomic model correctly captures the atomic rearrangements and plastic behavior of SMA-MG composite so that it is extensively applied for characterization of MGs and SMAs in the simulation studies [32]. Under the tensile loading, the atoms with  $\eta_{\text{Mises}} > 0.2$  were considered as the inelastic shear events, which are responsible for the formation of shear transformation zones (STZs) [35]. Through the adaptive common neighbor analysis, which is implemented in the open visualization tool, the structural transformation in the crystalline part of the system was monitored. The periodic boundary condition in the directions  $x$ ,  $y$ , and  $z$  was applied to omit any surface effect. The tensile test of specimens was conducted at 350 K perpendicular to the laminates with strain rate of  $1.2 \times 10^8 \text{ s}^{-1}$ . All the simulations were performed by the parallel program code and verified by the large-scale atomic massively parallel simulator software.

### 3. Results and Discussion

Figure 2 represents the stress-strain curves of SMA, MGs, and their composites under the tension mode. As observed, there exists a significant difference in the stress-strain curves of monolithic MGs and the SMA. However, one can see that the trend of the SMA-MG composites and the monolithic SMA is similar so that two major strain hardening events were detected in the plastic deformation stage of both states. On the other side, the monolithic MG shows a decreasing trend after the maximum pronounced stress (see Figure 2(a)). This event is associated to the formation and propagation of main shear bands in the alloying system. However, it is clear that the subtractive trend strongly relies on the MG composition. With the increase of Zr content, the monolithic MG tends to show a smoother behavior, which means that the plastic deformation comprises numerous interactive shear events [27, 36]. Moreover, the stress-strain curves showed that the tensile strength of monolithic CuZr MGs is considerably lower than the B2-CuZr SMA. This event is due to the fact that the small sample size and the high strain rate of loading in the MD simulation change the results than that of the experimental works [37]. At the small sizes, the surface stresses come into the play and affect the strength of material. As also reported in other works, this event is more intensified in the SMAs, compared with the amorphous alloys [27, 31].

Focusing on the SMA-MG composite (see Figure 2(b)), it is found that the stress-strain curve experiences some distinct stages with different stress levels. In general, the flow stress of SMA-MGs is much higher than the monolithic

MGs, suggesting that the martensitic transformation in the SMA leads to the increase of strength and plastic deformation capability in the alloying system [38]. Similar to the monolithic SMA, the composites exhibited a moderate stress increment after the martensitic transformation, which is a sign of strain hardening in the system. Thereafter, a stress drop occurs at the strain of 8–10% and then a fluctuated trend appears in the range of 10%–22%. Moreover, a further strain hardening is detected in the strain range of 22–25%. The intensity of this event strongly depends on the chemical composition of MG alloy, which indicates the importance of SMA and MG synergetic interaction during the tensile loading of composite. In general, the second strain hardening in the composite is originated from the completion of martensitic transformation from  $R$  to BCT phase in the SMA [27]; however, the restriction of SMA part by the MG affects the position and the degree of strain hardening in the composite.

The stress-strain curves provide important information regarding the mechanical properties of samples; however, it is still needed to characterize the plastic deformation portion of each phase in the composite. Figure 3 illustrates the fraction of atomic rearrangements with the  $\eta_{\text{Mises}} > 0.2$  in the MGs, SMA, and their composites. The previous studies confirmed that the sheared atomic rearrangements lead to the plastic deformation, when the Von-Mises strain exceeds 0.2 [31]. As observed, the 0.2-Von-Mises atomic rearrangement is negligible at the tensile strain less than 5% and 7% in the MGs and SMA, respectively. However, the increase in tensile strain leads to the beginning of sheared atomic rearrangement in the alloying systems. Considering the SMA part of composite, one can see that the sheared atomic strain exhibited a very slight increment in the range of 7–10% and then sharply increases up to 19–21% tensile strain. Afterwards, a steady state occurs in the range of 21–22%, and finally, an acute decrease is detected. It is believed that the slight increase of 0.2-Von-Mises atomic rearrangement in the range of 7–10% tensile strain is correlated to the first martensitic transformation from B2 to stable  $R$  phase, while the sharp atomic rearrangement at the tensile strain of 19–21% is caused by the martensitic transformation from the stable  $R$  phase to unstable body-centered tetragonal phase [32, 39]. On the other side, the MG part of composites behaves differently under the evolution of tensile loading. Compared to the SMA, the 0.2-Von-Mises atomic rearrangement in the MGs slightly increases in the range of 5–8% tensile strain and then a steady increment occurs in the structure, which is much moderate than the

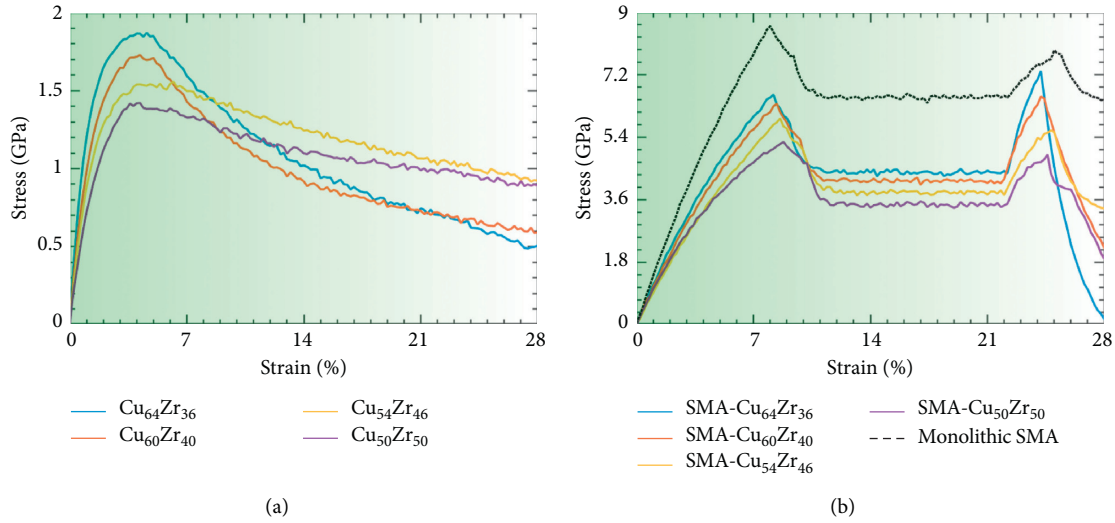


FIGURE 2: Stress-strain curves of (a) monolithic MGs and (b) monolithic SMA and the composites.

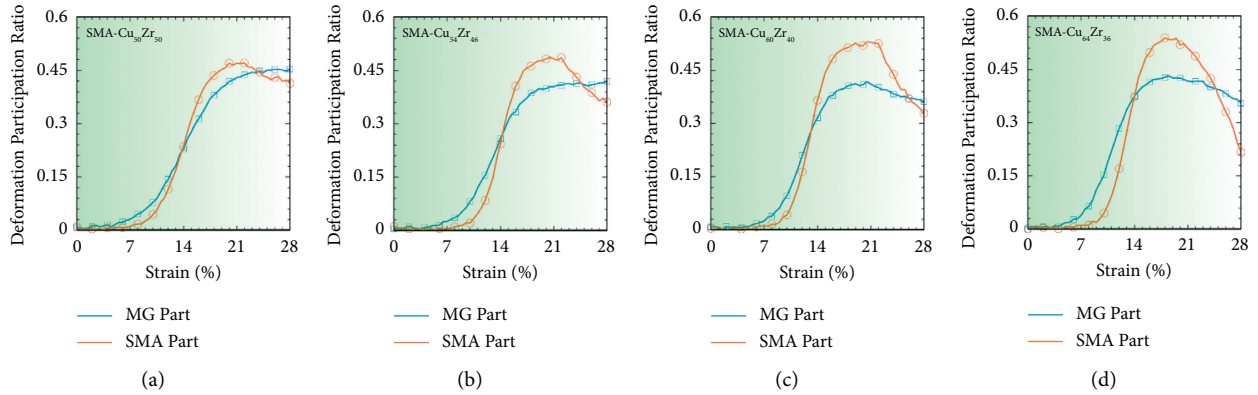


FIGURE 3: The deformation participation ratio based on  $\eta_{\text{Mises}} > 0.2$ .

SMA part. Moreover, it is found that the chemical composition of MG plays a significant role in the trend of the strain hardening event at the end of tensile test in the strain range of 21–28%. As observed, the increase in Zr content of MGs leads to the stable atomic rearrangement at the end of tensile loading so that a slight decrement is detected in the 0.2-strained atoms. On the other side, the Cu-rich MGs show a sharp Von-Mises strain decrement at the final stage, which is correlated to the catastrophic propagation of main shear bands in the system. Another interesting point is the dependency of strained-atom ratios in the SMA part of the composites to the MG compositions. Hence, it is concluded that the mechanism of deformation in the MG part significantly affects the plastic behavior of SMA part in the composite. This phenomenon will be discussed in detail.

The evolution of plastic deformation under the tensile loading was evaluated using the common neighbor analysis. Figure 4 demonstrates the snapshots of atomic configurations in the SMA-MG composite fabricated by the  $\text{Cu}_{60}\text{Zr}_{40}$  glassy alloy. Considering the MG part of composite, only the atoms with  $>0.2$  Von-Mises strain appeared in the snapshots

to better understand the evolution of plasticity at the body and interfaces of MG and SMA. Figure 4(a) represents the strain distribution at the first peak ( $\epsilon = 7\%$ ), in which there are just some sporadic atomic rearrangements in the MG part and the stability of crystalline B2 phase in the SMA. With the increase in tensile strain (Figure 4(b),  $\epsilon = 11\%$ ), the nucleation of shear bands occurs in the MG part. It is believed that the nucleation of shear band in the MG is related to the blockage of SMA part for the plastic deformation in the amorphous region. On the contrary, the SMA experiences the martensitic transformation from B2 to R phase, which is manifested in the immediate stress drop of the stress-strain curve ( $\epsilon = 11\%$ ). As reported in other works [40], the B2-R phase transformation is created through a twinning event along the  $\{1\ 0\ 0\}$  plane. With the rise of tensile strain (Figure 4(c),  $\epsilon = 14.8\%$ ), the B2-R transition is completed, which leads to a volume expansion in the SMA part and a subsequent pressure to the MG region. As a result, a plastic deformation zone at the interface of amorphous-crystalline phases is created and the potential sites for the formation and percolation of STZs increase in the MG

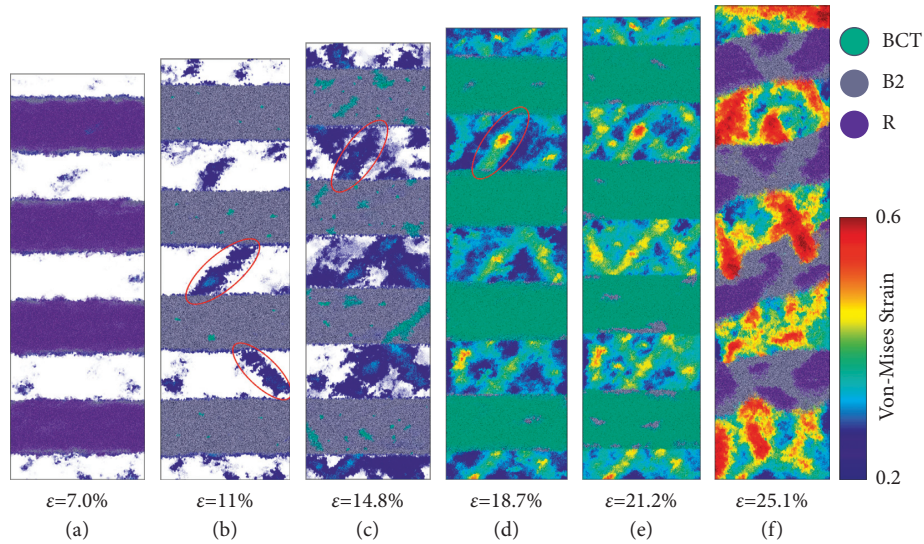


FIGURE 4: The atomic configurations of the composite fabricated by the  $\text{Cu}_{60}\text{Zr}_{40}$  MG under the evolution of tensile loading ((a)–(f)).

system. It is worth mentioning that the B2-R martensitic transformation does not include significant 0.2-Von Mises strains, which means that the B2-R transition is just a small-scale atomic rearrangement in the SMA system [41]. With the rise in the tensile strain (see Figures 4(d) and 4(e)), the percolation of STZs and formation of shear bands along the body of glassy alloy is intensified; however, there is still no sign of dominant shear band propagation in the material. This event is mainly due to the volume expansion of SMA under the martensitic transition. Moreover, it is suggested that the dissipation of energy in the crystalline phase transition inhibits the extensive percolation of STZs in the vicinity of interface [41]. Thereafter, the continuous strain increment leads to another martensitic transformation from R to BCT [27], which is clearly demonstrated in Figures 4(d) and 4(e). In this state, an increase of Von Mises strain occurs in the atoms of SMA, which indicates that the unstable BCT phase is originated from a high strain atomic rearrangements, i.e., a twinning event along the  $\{1\ 1\ 0\}$  plane [39]. This result is also consistent with that presented in Figure 3. With the completion of martensitic transition, the shear bands are eventually intensified in the MG part so that they break the interface and move into the SMA, which leads to the collapse of crystalline structure (see Figure 4(f)). This event induces the inverse martensitic transformation in the crystalline system and facilitates the shear band propagation, which is consistent with the eventual stress drop in the stress-strain curve. In total, one can conclude that the SMA is mostly responsible for the prevention of sudden shear banding propagation in the MG alloy. It should be noted that the design of SMA-MG interface plays a crucial role in the mechanism of plastic deformation in the laminated composite, especially where the loading direction is perpendicular to the SMA-MG interfaces. As performed in this work, the periodic boundary conditions lead to the capture of shear events at the interfaces and the inhabitation of shear banding at the free surfaces [42]. Under this condition, the laminated composite is stretched perpendicular to the

interface planes and the stress normal to the tensile loading becomes relaxed and induces a lateral contraction. This event is clearly seen in the evolution of snapshots sizes under the tensile loading (see Figure 4).

As depicted in Figure 2, the MG composition plays a crucial role in the plasticity evolution of composites under the tensile loading. For this reason, the final stage of plastic deformation in the composites with different MG compositions should be explained in detail. Figure 5 shows the snapshots of atomic configuration of composites fabricated with different MG compositions at the end stage of tensile loading. As illustrated in the figure, the Cu-rich MG ( $\text{Cu}_{64}\text{Zr}_{36}$  and  $\text{Cu}_{60}\text{Zr}_{40}$ ) facilitates the formation of thick shear bands in the structure, leading to a more catastrophic failure in the composite. In other words, the thicker shear bands intensify the localized deformation and induce the sudden atomic rearrangement in the SMA part of composite. With the increase of Zr content ( $\text{Cu}_{54}\text{Zr}_{46}$ ), the localized deformation decreases in the MG region and the plasticity mechanism is defined by the homogeneous nucleation of STZs and the creation of more fine shear bands in the system. This event is the main reason for the inhabitation of sudden stress drop at the end of the stress-strain curve, compared to the Cu-rich MG composites (See Figure 2). Nevertheless, the excessive rise of Zr content ( $\text{Cu}_{50}\text{Zr}_{50}$ ) leads to the formation of percolated defects in the composite system. As observed in Figure 5, the plastic deformation of Zr-rich MG significantly proceeds before the complete evolution of martensitic transformation in the SMA part at the end of tensile loading. This event implies that the deformed MG applied insufficient energy on the SMA to provide the driving force for the martensitic transformation. Consequently, one can see that there exist some sporadic regions in the SMA part facing with the inverse martensitic transition at the end of tensile loading. Furthermore, instead of shear band propagation, the plasticity of Zr-rich MG strongly depends on the extension of STZs in the structure. As a result, the MG part absorbs a large amount of strain

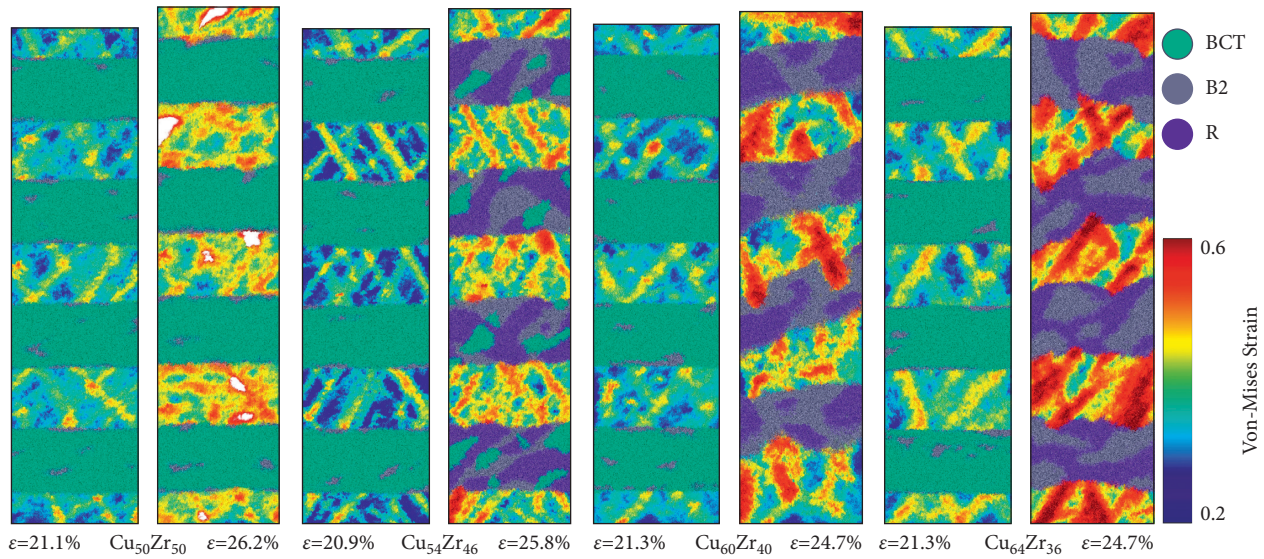


FIGURE 5: The atomic configurations of the composites at the end stage of tensile loading.

energy under the tensile loading, which intensifies the agglomeration of high-strained atoms and the extra local softened regions at the interface. In other words, the excessive softened structure of Zr-rich MG hampers the typical propagation of shear bands into the SMA part. This event is the main factor for the creation and aggregation of nanoscale pores at the SMA/MG interface. The spaces with less than 5% of average atomic density were considered as a criterion for the aggregation of nanopores in the structure. These pores are the main reasons for the deterioration of mechanical properties in the composites fabricated by  $\text{Cu}_{50}\text{Zr}_{50}$ . Accordingly, it is believed that an optimized alloying composition is needed for the maximum homogenous plasticity and superior mechanical properties in the SMA-MG composites. It is also important to discuss the mechanism of shear banding in the composite systems based on the stress distribution. In general, the surrounding stress fields determine the features of shear banding in the amorphous alloys [43, 44]. This fact is highlighted in our work, where the MG size is very small in the laminated composite and confined by the SMA part. As a result, the localized complex stress fields affect the distribution of shear events in the amorphous part. It is suggested that the localized stress fields are intensified in the Cu-rich MGs, leading to the lower elastic limit in the stress-strain curves (see Figure 2). On the other side, the increase in Zr content leads to the more homogenous distribution of atomic strains in the MG structure, impeding the creation of embryonic shear bands after the yielding event. Consequently, one can see that the composites with Cu-rich MGs tend to propagate the dominant shear bands during the tensile loading. This result is also consistent with other works reporting the easily localized atomic strains in the confined and thin layer Cu-rich MGs, leading to the visible shear band under an external loading [45].

Figure 6 illustrates the von Mises strain snapshots of monolithic MGs at the final stage of tensile loading. As can

be seen, the evolution of plastic deformation in the monolithic MGs is completely different from that occurred in the laminated composites. The dominance of shear band across the sample and the necking event at the center part are the signs of deformation under the tension. Nevertheless, one can observe that the increase in Cu content intensifies the shear banding and induces the percolation of shear events in the structure. On the other side, the rise of Zr content inhibits the catastrophic shear band propagation, which is due to the presence of numerous potential sites for the STZ formation in the structure [46].

The Voronoi analysis was also carried out to further characterize the role of MG composition on the final properties of composites. Using this method, it is possible to find out the atomic rearrangement and local structure variations in the glassy system [47]. In general, the Voronoi tessellation characterizes the polyhedrons according to the indices  $\langle n_{i3}, n_{i4}, n_{i5}, n_{i6} \rangle$ , in which the “ $n_i$ ” parameter determines the polyhedron  $i$ -edged faces. Figure 7 illustrates the evolution of main polyhedrons during the tensile loading for the MG part of the composites. Although the initial percentage of polyhedron types is different in each alloying composition, it is clear that the polyhedrons  $\langle 0, 2, 8, 1 \rangle$  and  $\langle 0, 0, 12, 0 \rangle$  are the dominant short-range structures in all the MGs. As given in Figure 7(a), the polyhedrons  $\langle 0, 2, 8, 1 \rangle$  and  $\langle 0, 0, 12, 0 \rangle$  are sharply decreased in the  $\text{Cu}_{64}\text{Zr}_{36}$  during the tensile loading; however, there is a significant rise of polyhedrons  $\langle 0, 3, 6, 3 \rangle$  and  $\langle 0, 1, 10, 2 \rangle$  in the system. Moreover, the polyhedron  $\langle 0, 2, 8, 2 \rangle$  exhibits a stable trend under the tensile loading. This event with a slighter trend was also detected in the SMA- $\text{Cu}_{60}\text{Zr}_{40}$  composite. Consequently, it was suggested that the formation and propagation of thick shear bands in the MG structure led to the sharp annihilation of the polyhedrons  $\langle 0, 2, 8, 1 \rangle$  and  $\langle 0, 0, 12, 0 \rangle$  and the marked increment of polyhedrons  $\langle 0, 3, 6, 3 \rangle$  and  $\langle 0, 1, 10, 2 \rangle$  in the system. On the other side, the increase in Zr content ( $\text{Cu}_{54}\text{Zr}_{46}$  and  $\text{Cu}_{50}\text{Zr}_{50}$ ) prevents the sharp

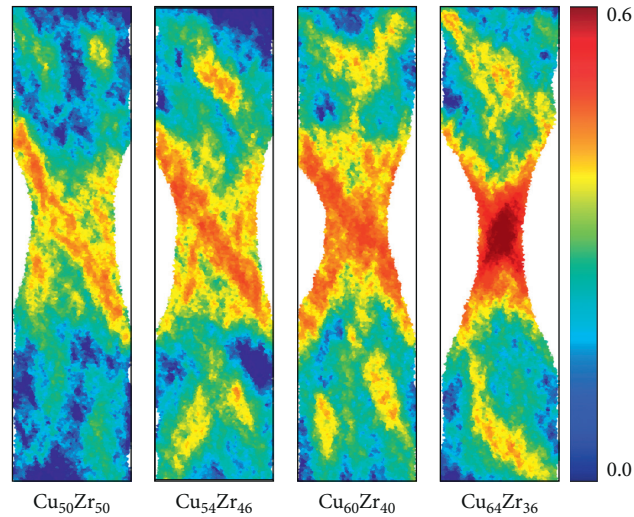


FIGURE 6: The atomic configurations of the monolithic MGs at the end stage of tensile loading. The strain value for  $\text{Cu}_{50}\text{Zr}_{50}$ ,  $\text{Cu}_{54}\text{Zr}_{46}$ ,  $\text{Cu}_{60}\text{Zr}_{40}$ , and  $\text{Cu}_{64}\text{Zr}_{36}$  is 26.2%, 25.8%, 24.7%, and 24.8%, respectively.

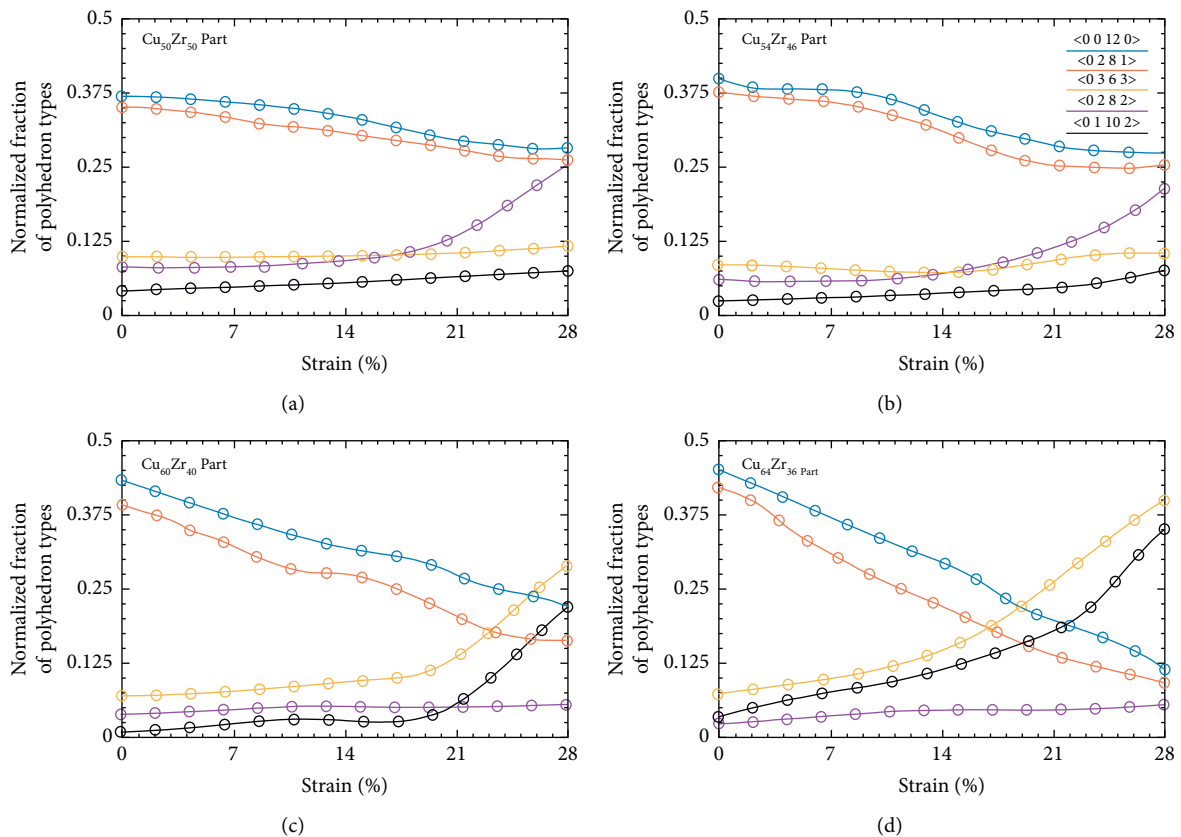


FIGURE 7: The evolution of polyhedron types during the tensile loading in the MG part of composites fabricated by (a)  $\text{Cu}_{50}\text{Zr}_{50}$ , (b)  $\text{Cu}_{54}\text{Zr}_{46}$ , (c)  $\text{Cu}_{60}\text{Zr}_{40}$ , and (d)  $\text{Cu}_{64}\text{Zr}_{36}$ .

annihilation/formation of polyhedrons in the glassy structure. Moreover, it was found that the creation of polyhedron  $\langle 0, 2, 8, 2 \rangle$  is intensified in the Zr-rich MGs under the evolution of tensile loading. As a result, it is suggested that the nucleation of STZs with sporadic distribution strongly

relies on the appearance of polyhedron  $\langle 0, 2, 8, 2 \rangle$  in the Zr-rich system; while the percolation of STZs, especially occurred in Cu-rich MGs, is accompanied with sharp formation of polyhedrons  $\langle 0, 3, 6, 3 \rangle$  and  $\langle 0, 1, 10, 2 \rangle$ . In summary, it is concluded that the evolution of tensile strain

strongly depends on the alloying composition of MGs so that a slight alteration leads to a marked effect on the mechanical behavior of material. Finally, it is suggested that the composite with  $\text{Cu}_{54}\text{Zr}_{46}$  MG represents the optimized plastic deformation behavior.

#### 4. Conclusion

This work aims to tune the mechanical properties and plasticity behavior of SMA-MG composites through the change of the glass composition. For this purpose, laminated nanostructures with the crystalline B2-CuZr and  $\text{Cu}_{50}\text{Zr}_{50}$ ,  $\text{Cu}_{54}\text{Zr}_{46}$ ,  $\text{Cu}_{60}\text{Zr}_{40}$ , and  $\text{Cu}_{64}\text{Zr}_{36}$  MGs were designed by the MD simulation. The results are as follows:

- (1) The martensitic transformation in the SMA restricted the sudden shear band propagation in the composite for all the specimens.
- (2) The composites which comprised of  $\text{Cu}_{60}\text{Zr}_{40}$  and  $\text{Cu}_{64}\text{Zr}_{36}$  MGs exhibited a higher strength; however, their plastic deformation is accompanied with the formation of thick shear bands at the end of tension loading.
- (3) The mechanism of plastic deformation in the SMA- $\text{Cu}_{54}\text{Zr}_{46}$  composite is based on the formation of finer shear bands with multiple interactive events, leading to a more homogeneous plasticity. Nevertheless, the extra addition of Zr content ( $\text{Cu}_{50}\text{Zr}_{50}$ ) facilitated the aggregation of nanopores at the interface of SMA and MGs, deteriorating the mechanical properties. As a result, it is suggested the optimized MG composition leads to a trade-off between the strength and plasticity in the SMA-MG composites.

#### Data Availability

The data used to support the findings of the study are available from the corresponding author upon request.

#### Conflicts of Interest

The authors declare that they have no conflicts of interest.

#### References

- [1] S. Scudino, J. J. Bian, H. Shakur Shahabi et al., "Ductile bulk metallic glass by controlling structural heterogeneities," *Scientific Reports*, vol. 8, no. 1, p. 9174, 2018.
- [2] Z. Zhang, J.-h. Zhang, J. Wang et al., "Toward the development of Mg alloys with simultaneously improved strength and ductility by refining grain size via the deformation process," *International Journal of Minerals, Metallurgy and Materials*, vol. 28, no. 1, pp. 30–45, 2021.
- [3] M. Samavatian, R. Gholamipour, and V. Samavatian, "Discovery of novel quaternary bulk metallic glasses using a developed correlation-based neural network approach," *Computational Materials Science*, vol. 186, Article ID 110025, 2021.
- [4] T. Wang, L. Zhang, Q. Hou, Q. Hao, and J. Qiao, "Improvement the plasticity of Fe-based bulk metallic glass via low temperature annealing," *Journal of Non-crystalline Solids*, vol. 569, Article ID 120965, 2021.
- [5] T. Ju and H. Zhou, "Pressure-induced maximum shear strength and transition from shear banding to uniform plasticity in metallic glass," *Extreme Mechanics Letters*, vol. 41, Article ID 101058, 2020.
- [6] H. C. Sun, Z. L. Ning, G. Wang et al., "In-situ tensile testing of ZrCu-based metallic glass composites," *Scientific Reports*, vol. 8, no. 1, Article ID 4651, 2018.
- [7] J. S. Langer, "Brittle-ductile transitions in a metallic glass," *Physical Review E*, vol. 101, no. 6, Article ID 63004, 2020.
- [8] Y. S. Luo, Z. Wang, and J. W. Qiao, "Flow serrations of rejuvenation behaviour through cryogenic thermal cycling for Zr-based bulk metallic glass," *Philosophical Magazine A*, vol. 101, pp. 1–12, 2021.
- [9] M. Samavatian, R. Gholamipour, V. Samavatian, and F. Farahani, "Effects of Nb minor addition on atomic structure and glass forming ability of Zr55Cu30Ni5Al10 bulk metallic glass," *Materials Research Express*, vol. 6, Article ID 65202, 2019.
- [10] S. Zhang, B. Shi, J. Wang, Y. Xu, and P. Jin, "Rejuvenation of a naturally aged bulk metallic glass by elastostatic loading," *Materials Science and Engineering: A*, vol. 806, Article ID 140843, 2021.
- [11] F. Dong, Y. Chu, M. He et al., "Manipulating internal flow units toward favorable plasticity in Zr-based bulk-metallic glasses by hydrogenation," *Journal of Materials Science & Technology*, vol. 102, 2021.
- [12] M. Samavatian, R. Gholamipour, A. A. Amadeh, and S. Mirdamadi, "Extra rejuvenation of Zr55Cu30Al10Ni5 bulk metallic glass using elastostatic loading and cryothermal treatment interaction," *Journal of Non-crystalline Solids*, vol. 506, pp. 39–45, 2019.
- [13] Y. Du, W. Han, Q. Zhou et al., "Enhancing the plasticity of a Ti-based bulk metallic glass composite by cryogenic cycling treatments," *Journal of Alloys and Compounds*, vol. 835, Article ID 155247, 2020.
- [14] Y. Lu, S. Su, S. Zhang et al., "Controllable additive manufacturing of gradient bulk metallic glass composite with high strength and tensile ductility," *Acta Materialia*, vol. 206, Article ID 116632, 2021.
- [15] W. J. Gao, W. W. Zhang, T. Zhang et al., "Large tensile plasticity in Zr-based metallic glass/stainless steel interpenetrating-phase composites prepared by high pressure die casting," *Composites Part B: Engineering*, vol. 224, Article ID 109226, 2021.
- [16] N. Li, J. Zhang, W. Xing, D. Ouyang, and L. Liu, "3D printing of Fe-based bulk metallic glass composites with combined high strength and fracture toughness," *Materials & Design*, vol. 143, pp. 285–296, 2018.
- [17] L. Zhang, R. L. Narayan, B. A. Sun et al., "Cooperative shear in bulk metallic glass composites containing metastable  $\beta$ -Ti dendrites," *Physical Review Letters*, vol. 125, no. 5, Article ID 55501, 2020.
- [18] J.-Z. Jiang, D. Hofmann, D. J. Jarvis, and H.-J. Fecht, "Low-density high-strength bulk metallic glasses and their composites: a review," *Advanced Engineering Materials*, vol. 17, no. 6, pp. 761–780, 2015.
- [19] L. Zhang, R. L. Narayan, H. M. Fu et al., "Tuning the microstructure and metastability of  $\beta$ -Ti for simultaneous enhancement of strength and ductility of Ti-based bulk metallic glass composites," *Acta Materialia*, vol. 168, pp. 24–36, 2019.
- [20] J. Cheng, J. Wang, Y. Yun, J. Rui, W. Zhao, and F. Li, "A novel core-shell structure reinforced Zr-based metallic glass



- composite with combined high strength and good tensile ductility,” *Journal of Alloys and Compounds*, vol. 803, pp. 413–416, 2019.
- [21] G. J. Lyu, J. C. Qiao, J. M. Pelletier, L. Zhang, H. F. Zhang, and Y. Yao, “Dynamic mechanical behaviors of a metastable  $\beta$ -type bulk metallic glass composite,” *Journal of Alloys and Compounds*, vol. 819, Article ID 153040, 2020.
- [22] S. Jiang, S. Guo, Y. Huang et al., “In situ study of the shear band features of a CuZr-based bulk metallic glass composite,” *Intermetallics*, vol. 112, Article ID 106523, 2019.
- [23] P. Zhang, C. Zhang, D. Ouyang, and L. Liu, “Enhancement of plasticity and toughness of 3D printed binary Zr<sub>50</sub>Cu<sub>50</sub> bulk metallic glass composite by deformation-induced martensitic transformation,” *Scripta Materialia*, vol. 192, pp. 7–12, 2021.
- [24] W. T. Jhou, C. Wang, S. Li, and C. H. Hsueh, “Nanoscaled superelastic behavior of shape memory alloy/metallic glass multilayered films,” *Composites Part B: Engineering*, vol. 142, pp. 193–199, 2018.
- [25] X. Zhang, J. Ren, and X. Ding, “Synergistic effects among the structure, martensite transformation and shear band in a shape memory alloy-metallic glass composite,” *Applied Composite Materials*, vol. 26, no. 2, pp. 455–467, 2019.
- [26] D. Şopu, X. Yuan, F. Moitzzi, M. Stoica, and J. Eckert, “Structure–property relationships in shape memory metallic glass composites,” *Materials*, vol. 12, Article ID 1419, 2019.
- [27] W. W. Li, H. Y. Song, J. L. Dai, J. Y. Wang, M. R. An, and Y. L. Li, “Effect of shape memory alloys on the mechanical properties of metallic glasses: a molecular dynamics study,” *Computational Materials Science*, vol. 187, Article ID 110088, 2021.
- [28] X. Fu, G. Wang, Y. Wu et al., “Compressive ductility and fracture resistance in CuZr-based shape-memory metallic-glass composites,” *International Journal of Plasticity*, vol. 128, Article ID 102687, 2020.
- [29] W. Guo, T. Wada, and H. Kato, “Work-hardenable Mg-based bulk metallic glass matrix composites reinforced by ex-situ porous shape-memory-alloy particles,” *Materials Letters*, vol. 183, pp. 454–458, 2016.
- [30] S. Gouripriya and P. Tandaiya, “Mechanistic origins of work hardening in shape memory alloy particle reinforced ex-situ bulk metallic glass matrix composites,” *Scripta Materialia*, vol. 185, pp. 1–6, 2020.
- [31] D. Şopu, K. Albe, and J. Eckert, “Metallic glass nanolaminates with shape memory alloys,” *Acta Materialia*, vol. 159, pp. 344–351, 2018.
- [32] D. Şopu, M. Stoica, and J. Eckert, “Deformation behavior of metallic glass composites reinforced with shape memory nanowires studied via molecular dynamics simulations,” *Applied Physics Letters*, vol. 106, Article ID 211902, 2015.
- [33] S. Yuan, X. Song, and P. S. Branicio, “Tuning the mechanical properties of shape memory metallic glass composites with brick and mortar designs,” *Scripta Materialia*, vol. 186, pp. 69–73, 2020.
- [34] M. I. Mendeleev, D. J. Sordelet, and M. J. Kramer, “Using atomistic computer simulations to analyze x-ray diffraction data from metallic glasses,” *Journal of Applied Physics*, vol. 102, Article ID 43501, 2007.
- [35] F. Shimizu, S. Ogata, and J. Li, “Theory of shear banding in metallic glasses and molecular dynamics calculations,” *Materials Transactions*, vol. 48, no. 11, pp. 2923–2927, 2007.
- [36] R. Rezaei, M. Shariati, H. Tavakoli-Anbaran, and C. Deng, “Mechanical characteristics of CNT-reinforced metallic glass nanocomposites by molecular dynamics simulations,” *Computational Materials Science*, vol. 119, pp. 19–26, 2016.
- [37] X. Zhou, H. Zhou, X. Li, and C. Chen, “Size effects on tensile and compressive strengths in metallic glass nanowires,” *Journal of the Mechanics and Physics of Solids*, vol. 84, pp. 130–144, 2015.
- [38] N. Amigo, “Martensitic transformation induced by void defects in the B2-CuZr crystal structure: an atomistic analysis,” *Molecular Simulation*, vol. 45, no. 12, pp. 951–957, 2019.
- [39] V. K. Sutrar and D. R. Mahapatra, “Designing copper-zirconium based nanowires for improving yield strength and plasticity by configuring surface atoms,” *Journal of Nanoparticle Research*, vol. 13, no. 12, pp. 6907–6918, 2011.
- [40] V. K. Sutrar and D. R. Mahapatra, “Single and multi-step phase transformation in CuZr nanowire under compressive/tensile loading,” *Intermetallics*, vol. 18, no. 4, pp. 679–687, 2010.
- [41] N. Amigo, M. Sepúlveda-Macías, and G. Gutiérrez, “Martensitic transformation to monoclinic phase in bulk B2-CuZr,” *Intermetallics*, vol. 91, pp. 16–21, 2017.
- [42] D. Şopu and K. Albe, “Influence of grain size and composition, topology and excess free volume on the deformation behavior of Cu–Zr nanoglasses,” *Beilstein Journal of Nanotechnology*, vol. 6, pp. 537–545, 2015.
- [43] Z. T. Wang, J. Pan, Y. Li, and C. A. Schuh, “Densification and strain hardening of a metallic glass under tension at room temperature,” *Physical Review Letters*, vol. 111, no. 13, Article ID 135504, 2013.
- [44] S. H. Chen, H. H. Tang, H. M. Zheng et al., “Achieving stable plastic flows in a Zr-based bulk metallic glass under tailored mixed-mode (I/II) loading conditions,” *Materials Science and Engineering: A*, vol. 772, Article ID 138695, 2020.
- [45] S. H. Chen, T. Li, W. J. Chang et al., “On the formation of shear bands in a metallic glass under tailored complex stress fields,” *Journal of Materials Science & Technology*, vol. 53, pp. 112–117, 2020.
- [46] M. Tercini, R. Gomes de Aguiar Veiga, and A. Zúñiga, “Structural changes and kinetics of shear banding in metallic glass composites,” *Journal of Alloys and Compounds*, vol. 819, Article ID 153046, 2020.
- [47] M. Kbirou, S. Trady, A. Hasnaoui, and M. Mazroui, “Short and medium-range orders in Co<sub>3</sub>Al metallic glass,” *Chemical Physics*, vol. 513, pp. 58–66, 2018.